Quaternary International 302 (2013) 199–209

Contents lists available at SciVerse ScienceDirect

Quaternary International

journal homepage: www.elsevier.com/locate/quaint

Study of variation in groundwater quality in a coastal aquifer in north-eastern Tunisia using multivariate factor analysis

Sihem Charfi [a,*], Kamel Zouari [a], Saber Feki [b], Ezeddine Mami [c]

[a] University of Sfax, National School of Engineers, Laboratory of Radio-Analyses and Environment, B.P1173-3038 Sfax, Tunisia
[b] University of Science and Technology (KAUST), Thuwal, Jeddah 23955, Saudi Arabia
[c] Regional Commissary for Agricultural Development of Nabeul, Nabeul, Tunisia

ARTICLE INFO

Article history:
Available online 3 November 2012

ABSTRACT

This work focuses on the Grombalia aquifer which constitutes the main water resource in Northeast Tunisia, Cap Bon Peninsula. The recharge of this aquifer is ensured mainly by direct infiltration of rainwater through permeable layers.

Under semi-arid climatic conditions and increasing water demand for irrigation, about 80% of the Grombalia aquifer system shows different vulnerabilities to anthropogenic activities. The total dissolved solids values range from 0.75 to 5.6 g/l.

Isotopic characterization with stable isotopes (δ^2H and $\delta^{18}O$) of Grombalia aquifer system identified geochemistry processes that control water chemistry. In addition, the multivariate statistical technique (Principal Component Analysis) was used to identify the origin, the recharge mode and geochemical processes controlling groundwater quality. The principal reactions responsible for the hydrochemical evolution in the Grombalia groundwater fall into three categories: (1) denitrification process; (2) dissolution of salts; and (3) irrigation return flow process. Tritium data in groundwater from the study area suggest the existence of pre1950 and post1960 recharge.

1. Introduction

Groundwater quality could be influenced by many factors including climate, aquifer lithology, surface water recharge (Pulido Leboeuf, 2004), and waste water pollution. Principal component analysis (PCA) is a mathematical technique that is successfully applied to investigate problems in geological investigation, such as geochemistry (Chen et al., 2007), and environmental science (Liu et al., 2003). This statistical method has many advantages over classical graphical approaches as it takes into consideration a huge amount of spatial and temporal data of water quality. The main advantage of this method is the reduction of variables dimension by providing the correlation between measured chemical variables and their multivariate patterns based upon the correlation or covariance matrix (Helena et al., 2000). So, it is mainly used to group together different geochemical variables according to their degree of co-variation among samples. The geochemical interpretation of determined factors gives insights into the dominant processes influence groundwater chemistry (Chen et al., 2007). The aim of this study was the specification of regional groundwater and the mechanisms controlling the chemistry in the Grombalia area, using geochemical and isotopic tools.

2. Study area

The study area lies in the Cap Bon Peninsula of Tunisia and extends between 36° 29′ 00″–36° 42′ 00″N, 10° 27′ 00″–10° 47′ 00″E, about 719 km^2. It is located between the Bouchoucha and Halloufa Jebal in the west, Abderrahman Jebal in the east, the plains of Hammamet in the south, and the Gulf of Tunis in the north (Fig. 2).

Grombalia plain is characterized by a semi-arid to sub-humid Mediterranean climate. This type of climate is the result of the convergence of several climatic parameters: rainfall is variable in time and space, with an annual average value of 500 mm. The mean annual temperature is around 18.7 °C. The potential evapotranspiration, about 1200 mm/year, is higher in summer as a result of the increase in temperature and the decrease in the air moisture.

3. Geology and hydrogeology

The Cap Bon region contains a series of Quaternary terraces, marine and continental. The survey based on the geophysical data

* Corresponding author.
E-mail address: charfisihem1@yahoo.fr (S. Charfi).

1040-6182/$ – see front matter © 2012 Elsevier Ltd and INQUA. All rights reserved.
http://dx.doi.org/10.1016/j.quaint.2012.11.002

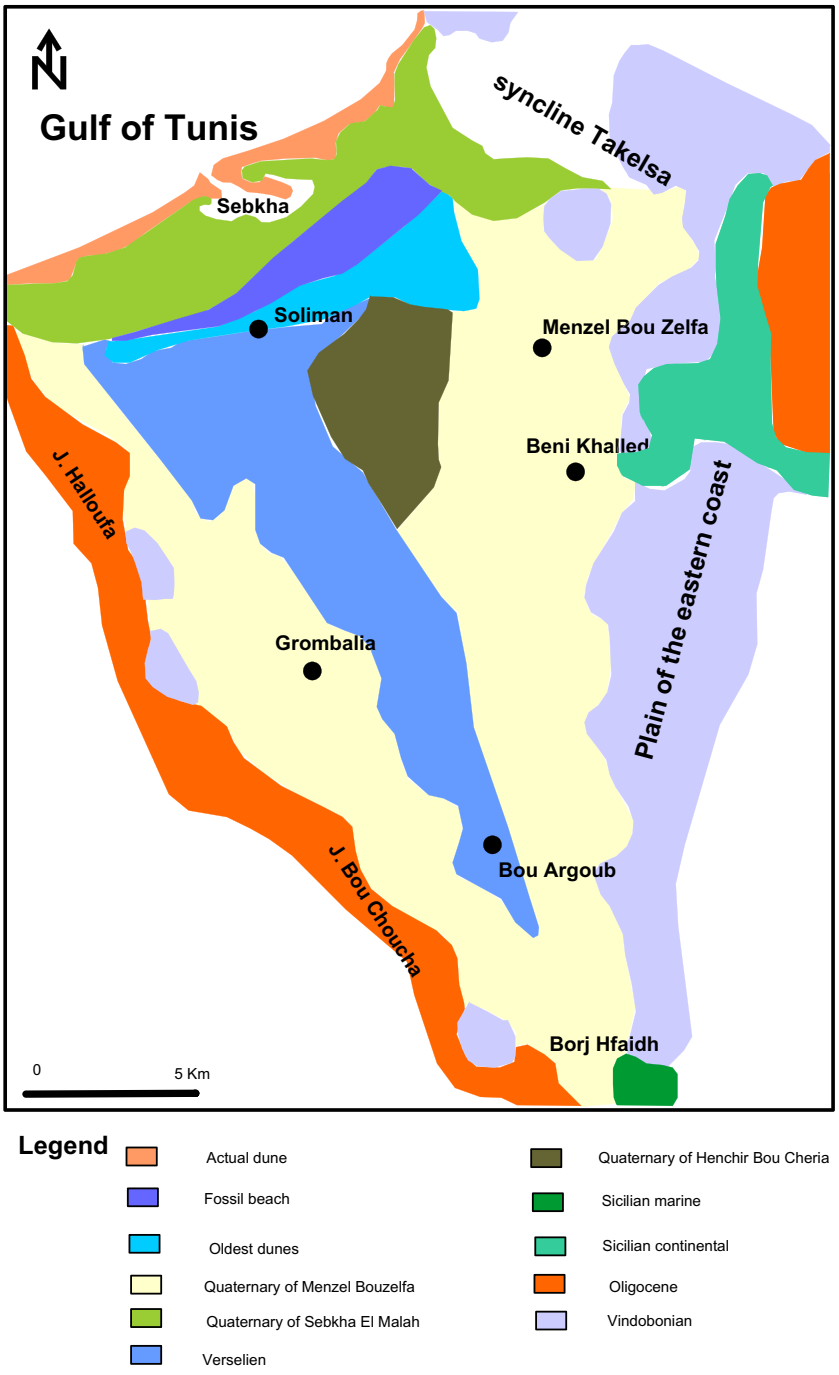

Fig. 1. Geological Map of the plain Grombalia (Castany, 1948 according to the Geological maps at 1:50.000).

and deep boreholes located in areas of Soliman, Menzel Bou Zelfa, Beni Khalled and Grombalia identified the following horizons (Schoeller, 1939) (Fig. 1):

- The Sicilian is represented by marine clay deposits in the southeast, and continental deposits containing gravel in the northeast;
- The Monastrien is composed of the following units: (i) The Quaternary lagoon of Henchir Bou Cheria, composed of deposits of coarse sands with marly intercalations; (ii) The Quaternary of the region of Soliman, formed by fossil beach composed of sand and very coarse sandstone, and the oldest dunes made of fine sand more or less consolidated, modal thickness of 20–35 m (Castany, 1948); (iii) The Quaternary sand of Menzel Bou Zelfa – Beni Khalled composed of yellow sands with some intercalations of sandstone; and (iv) The Quaternary of the plain of Sebkha El Malah, approximately 20 m silt.
- The Flandrian, mostly made up of yellow sands of the Quaternary up to a thickness of 23 m.

From a tectonic point of view, the folded structures of Jebel Abderrahman Korbous located at the northern limit of the Grombalia plain, attest to the collapse of the graben prior to folding.

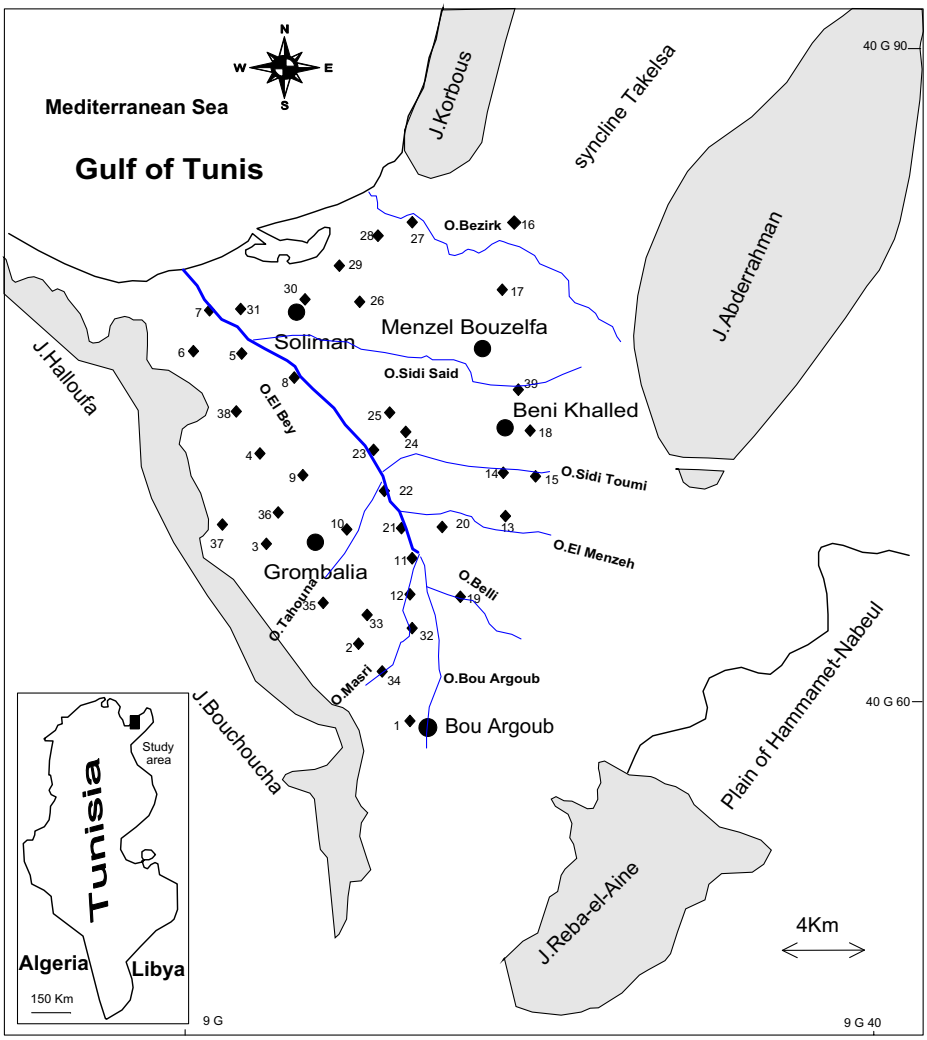

Fig. 2. Location and sampling map of the Grombalia plain.

Geologically, it is a small basin oriented NW–SE and filled by Quaternary sediment, the edges of which were related to two normal faults that appeared during the Middle Miocene (Hadj Sassi et al., 2006). These are the Borj cedria NNW–SSE normal fault and the Hammamet NE–SW normal fault (Ben Ayed, 1993; Ben Salem, 1995; Chihi, 1995). They contributed to the collapse of the plain, giving rise to the rift.

The Grombalia Graben is formed by subsidence of more than 500 m of Quaternary deposits. The Quaternary detrital sedimentation mainly consists of fine to coarse grained sands, clayey sands, sandstone, silt and abundant evaporate deposits (Schoeller, 1939; Colleuil, 1976; Ben Salem, 1995; Ben Moussa et al., 2010).

From a hydrogeologic point of view, the Grombalia shallow aquifer, with an average of about 50 m, is hosted in the Quaternary continental sand, clayey sand and sandstones deposits, which repose on 15 m-thick clay (Ben Moussa, 2011) (Fig. 3). The permeability values range from $5.4*10^{-6}$ to $6.5*10^{-3}$ (DGRE, 1990).

This aquifer represents the principal source of water supply. In 2009, the annual exploitation in the region was estimated at 250 Mm^3/year. The general direction of groundwater flow is toward the Gulf of Tunis from the relief of Jebel Abderrahman, Bouchoucha and Halloufa. In 2012, the value of piezometric level decline was 10 m.

The Miocene sandstone and clay series are found essentially in the eastern coastal hills and in some restricted areas along the foot of the Halloufa and Bouchoucha mountains (Ben Moussa et al., 2010). Previous studies have excluded hydrologic communication between the study area and the Takelsa syncline.

4. Materials and methods

For the evaluation of groundwater quality, 39 water samples were collected from the shallow aquifer of the Grombalia plain during June 2008. The groundwater samples were analysed for chemical and isotopic compositions. Measurement of temperature, conductivity and pH were measured in the field. Major elements (SO_4^{2-}, Cl^-, NO_3^-, Ca^{2+}, Mg^{2+}, Na^+, K^+) were analysed by ion liquid chromatography (HPLC) at the Laboratory of Radio-Analysis and Environment of the National School of Engineers of Sfax.

The total alkalinity (as HCO_3) was determined by titration with 0.1 N HCl solution using methyl orange indicator. Stable isotopes ($\delta^{18}O$, δ^2H) analyses were performed in the Laboratory of the International Agency of Atomic Energy (IAEA) in Vienna, using, respectively the standard CO_2 equilibration (Epstein and Meyada, 1953) and zinc reduction techniques (Coleman et al., 1982),

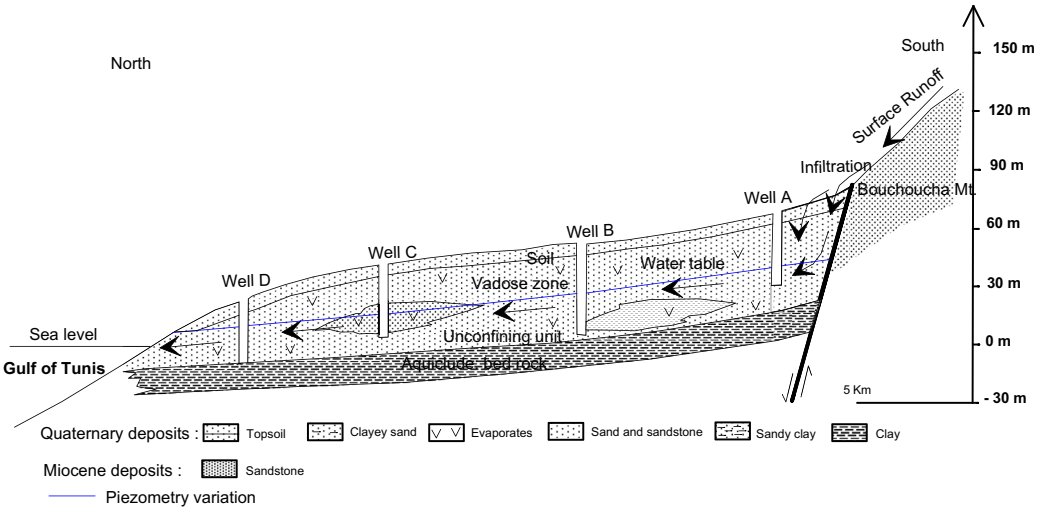

Fig. 3. Hydrogeological cross section of the Grombalia aquifer (Ben Moussa et al., 2010).

followed by an analysis on a mass spectrometer. The results are expressed as relative deviations δ (in per mil) from the Vienna standard mean ocean water (VSMOW). The analytical precision of stable isotope analyses (one sigma) was in the order of 0.1‰ for $\delta^{18}O$ and 1‰ for $\delta^{2}H$. All the statistical evaluations were carried out using XL STAT 2006 for windows.

The tritium content was measured at the IAEA laboratory using electrolytic enrichment and liquid scintillation spectrometry (Taylor, 1977). The results are expressed in Tritium Units (TU) with the analytical uncertainty in the order of 0.3 TU. The results of chemical analyses of the investigated groundwater samples are presented in Table 1.

Table 1
Geochemical data for the studied aquifers.

Well N°	EC (mS/cm)	T (°C)	pH	Na^+ (mg/l)	Ca^{2+} (mg/l)	Mg^{2+} (mg/l)	K^+ (mg/l)	Cl^- (mg/l)	SO_4^{2-} (mg/l)	NO_3^- (mg/l)	Alkalinity (mg/l)	TDS (mg/l)	I.B (%)
1	2.77	14.5	7.21	250.8	270.7	68.7	20.1	424.2	398.7	145	396.5	1974.5	2.5
2	3.7	16.4	7.04	243.9	220.2	109.2	62.9	399.4	493.7	64.3	390.2	1983.7	4.9
3	3.08	16.6	7.17	190	195.8	65	4.6	328.4	153.2	85.4	457.5	1479.8	4.9
4	2.77	15	7.19	207.7	228.1	77.7	3.2	523.2	193.4	82.1	390.4	1705.8	0.7
5	4.1	15.4	7.24	448.5	445.2	141.7	4.8	1020.2	588.1	68.4	390.4	3107.3	4.9
6	2.76	14.7	7.37	244.8	225.9	96.8	148.8	670	184	122.9	353.8	2047	5.0
7	1.821	17	7.53	130.6	119.9	55.7	3.9	330	160.4	64.1	231.8	1096.4	−3.3
8	5.01	12.9	7.86	800	289	180	9.5	1240	882	0.8	298.9	3700.3	4.9
9	5.18	13.4	7.61	766.4	241.5	235	17.9	1273.6	640	417.3	305	3896.7	3.3
10	4.38	16.5	7.37	569.6	269.7	297	5.1	999.4	1073.8	44.3	488	3746.9	2.9
11	6.65	15.5	7.09	568.8	495.4	365.5	7.7	2190.1	426.6	198.3	286.7	4539.2	0.8
12	5.6	13.9	7.23	660.2	423.3	342.1	6.9	1260	1295.3	86.1	420.9	4494.6	5.0
13	2.68	14.9	7.34	224.7	306.3	49.9	39.6	405	440.3	63.5	353.8	1883.1	4.9
14	3.54	14.8	7.33	261	447.9	133.1	18.5	656.8	725	108	427	2777.3	3.2
15	1.695	14.6	7.41	113.2	147.6	40.3	7	146	57.1	112.4	439.2	1062.8	4.9
16	3.73	17	7.1	346.4	414	122.3	14.8	774	617.5	137.4	500.2	2926.5	1.2
17	2.25	17.5	7.41	141.6	180	47.9	3.3	306.2	208.9	83.2	384.3	1355.4	−3.6
18	4.19	18.2	7.17	279.3	443.1	98.3	5.5	934.3	245.2	328.3	305	2638.8	0.9
19	1.419	17.6	7.92	130.5	139.9	95.3	9.4	372	138.9	51.1	280.6	1217.7	4.9
20	4.65	16.9	7.07	323	308.4	119.4	9.3	878.6	289.6	99.4	390.4	2418	0.9
21	7.84	17	7.09	696.1	525.8	440	19.2	2590.9	620.2	498	296.7	5686.8	−2.9
22	7.09	14.8	7.61	698.3	297.9	307.6	12	1510	766	123.8	451.4	4167	2.1
23	4.89	16	7.34	591.8	260.2	271.7	15.2	1150.5	1007.5	77	445.3	3819.2	−0.4
24	3.91	18.1	7.28	428.2	271	151	8.4	596	790.4	79.6	366	2690.6	5.0
25	2.5	18.5	7.27	233	294.3	114.7	3.9	596.6	472.4	79.4	366	2160.3	0.6
26	4.1	19.4	7.17	354.9	288.1	99.5	15.9	692.5	424.4	148.3	384.3	2407.7	1.8
27	3.55	21.2	7.33	754.2	550.5	153	14.3	1583	472.2	590	158.6	4275.7	4.8
28	1.122	18.4	7.64	828.1	412.6	165	8.1	1380	747.3	454	224	4219.1	3.6
29	5.22	18.3	7.29	170.1	300.6	44.3	21.4	384.6	320	109.1	378.2	1728.3	2.2
30	2.81	17.6	7.47	244.1	200.7	90.3	4	620.1	289.4	75.9	280.6	1805	−2
31	3.7	19.5	7.28	520	229.1	170	150.5	725.9	768.8	168	475.8	3208.1	5.0
32	3.65	15.9	7.5	326.8	313.4	174.5	4	850.8	557.5	13.9	292.8	2533.5	4.4
33	3.76	15.3	7.26	308.3	326.2	182.2	7.3	783	623.8	90.9	420.9	2742.4	1.6
34	4.16	16.8	7.02	406.4	296.9	105.3	7.4	695.5	479	66.7	414.8	2472.1	5.0
35	3.72	16.4	7.25	231.9	216.1	127.8	10.6	803.2	93.9	10	335.5	1829	2.3
36	2.57	16.2	7.53	210.2	295.7	79.4	4.7	463.7	292.7	99.5	460.6	1906.6	3.8
37	2.68	17.2	6.91	324.8	197.4	113.5	4.6	474.2	567.9	55.5	610	2347.8	−3.8
38	4.07	18.3	7.02	260.7	219.6	84.2	4.4	559.2	126	128	378.2	1760.3	4.8
39	1.817	11.9	7.63	73.3	138	20	4.4	173	79	35	231.8	754.5	4.2

5. Results and discussion

Temperature (T°), Electrical conductivity (EC), pH and major ion concentrations are summarized in Table 2. The pH ranges from 6.9 to 7.9 with an average value of 7.3. Independently of well depth, the temperature of groundwater samples varies significantly, from 11.9 °C to 21.2 °C.

Table 2
Statistical summary of hydrochemical parameters of groundwater samples.

Variable	Minimum	Maximum	Average	Std. dev
Cl	146.0	2590.9	814.5	520.9
NO_3	0.8	590.0	135.0	135.5
SO_4	57.1	1295.3	479.7	296.7
Alkalinity	158.6	610.0	370.8	88.8
Na	73.3	828.1	373.4	215.7
K	3.2	150.5	18.5	32.8
Mg	20.0	440.0	144.5	97.2
Ca	119.9	550.5	293.5	109.1
TDS	754.5	5686.8	2629.9	1145.6
EC	1100	7800	3700	1500
T °C	11.9	21.2	16.4	1.9
pH	6.9	7.9	7.3	0.2

pH (standard units), EC (μ Siemens/cm) and concentration (mg/l).

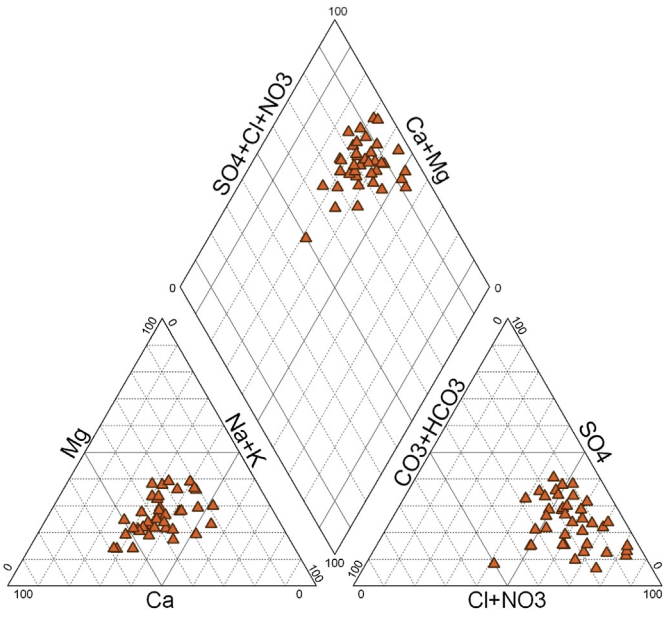

Fig. 4. Piper diagram of the aquifer groundwaters.

The total dissolved solids and the electrical conductivity (EC) values range from 754.5 to 5686.8 mg/l and 1100 to 7800 μ S/cm with average values of 2629.9 mg/l and 3700 μ S/cm (Table 2). These large variations in groundwater salinity could be influenced by different processes such as evaporation, anthropogenic activity, the interaction water–rock mixing processes. The order of the cation chemistry for are Na > Ca > Mg > K and all groundwater samples exceed the suitable limit of Ca for drinking water (75 mg/l) (WHO, 1993). The order of abundance of anion chemistry is Cl > SO_4 > HCO_3. All groundwater samples exceed the suitable limit of Cl (200 mg/l) for drinking water (WHO, 1993), except for sample P15 and P39, where Cl content is respectively 146 mg/l and 173 mg/l.

5.1. Major ion geochemistry

The Piper diagram (Piper, 1944) was determined to precisely recognize the different groundwater facies. Nitrate concentration was taken into account when plotting this diagram because of its relative abundance in the groundwater. The data represented in this diagram show that groundwater samples are classified into two major groups: (Ca_SO_4_Cl water type) and (Na_Cl_NO_3 water type) (Fig. 4). Both facies differ in the proportions of sodium and calcium. In the triangle of cations, some samples show the dominance of sodium whereas others show a tendency to pole mixed calcium. In the triangle of anions, samples indicate predominance of chloride with a slight tendency to the sulfate pole.

5.2. Origin of mineralization

The correlation matrix established between 12 hydrochemical variables (T°, EC, pH, TDS, Cl, NO_3, SO_4, Alkalinity, Na, Mg, Ca and K) (Table 3) was used to determine the relationship existing between these variables. This matrix indicates that: (i) high correlation ($r \geq 0.9$) between Cl, Na, Mg and TDS reflects the significant contribution of these elements to the acquisition of the mineralization of water; (ii) the high correlation between Na and Cl ($r = 0.82$) indicates that the dissolution of halite is an important process of mineralization; (iii) the positive correlation between Ca and NO_3 shows the effect of nitrogen fertilizers; (iv) the low correlation between Ca and SO_4 ($r = 0.43$) shows that the dissolution of sulfate minerals is clearly affected by the process of base exchange with clay minerals; and (v) positive relationship between nitrate and TDS indicates the presence of contamination from agriculture.

Table 3
Correlation matrix of the geochemical variables in Grombalia groundwater shallow aquifer.

Variables	Cl	NO_3	SO_4	Alkalinity	Na	K	Mg	Ca	TDS	EC	T°	pH
Cl	1											
NO_3	0.61	1										
SO_4	0.48	0.09	1									
Alkalinity	−0.27	−0.44	0.26	1								
Na	0.82	0.55	0.74	−0.15	1							
K	−0.05	0.05	0.03	0.11	0.02	1						
Mg	0.88	0.34	0.69	0.01	0.76	−0.03	1					
Ca	0.74	0.59	0.43	−0.18	0.57	−0.11	0.54	1				
TDS	0.93	0.58	0.75	−0.07	0.92	0.02	0.90	0.75	1			
EC	0.75	0.23	0.47	0.10	0.58	−0.02	0.78	0.52	0.72	1		
T°	0.03	0.35	−0.10	−0.07	0.01	0.07	−0.11	0.17	0.03	−0.10	1	
pH	−0.05	−0.04	0.03	−0.45	0.13	−0.05	−0.05	−0.27	−0.06	−0.27	−0.29	1

5.3. Principal component analysis

Pearson's correlation analysis was applied to the data in (Table 3) to quantitatively analyse and characterize the relationship between physico-chemical parameters contents in groundwater samples. Principal component analysis (PCA) is the most common multivariate statistical method used in geochemistry studies. In addition, it reduces data and extracts a smaller number of latent factors for analyzing relationships between the observed variables. The varimax rotation, applied in this study, is the most common type of PCA that produces more interpretable components.

The total number of components generated from a multivariate analysis indicates the total number of possible sources of variation in groundwater quality. The Principal component axes were rotated to make high component loadings higher and low component loadings lower, therefore enhancing the interpretation of the data. Factor loadings greater than 0.71 are typically considered as excellent, and those lower than 0.32 are very poor for interpretation (Garcia et al., 2004). According to this criterion, only factors with eigenvalues greater than or equal to 1 will be selected as possible sources of variance in the data (Kaiser, 1960). The reason for selecting the value of 1 is that a factor must have a variance at least as large as that of a single standardized original variable to be acceptable.

The PCA approach preserving only the first two factors that have the most important loading and excluding the less important ones (Davis, 1986; Kumar et al., 2006). The preserved two factors represent 61.51% of total samples variance (46.46% for F1 and 15.05% for F2) (Fig. 5).

In space variables, the F1 factor takes high positive loading for all major elements except for alkalinity and pH that shows a negative loading. This major factor describes mineralization of groundwater by water–soil/rock interaction.

In addition, the negative loading for pH that corresponds to high positive loading for the NO_3 may provide insight into the significance of the denitrification process in relation to the forest vegetation, relatively abundant in these regions (Ben Moussa et al., 2012).

The axis F2 opposes Mg^{2+}, Alkalinity and K^+ to temperature, pH and Ca^{2+}. This axis basically representing the calco-carbonic parameters, describes factor dilution of groundwater by water recharge and/or mineralization by water–soil/rock interaction.

The opposite evolution of Alkalinity (HCO_3^-) and Ca^{2+} in factor 2 indicates that the increase of Ca^{2+} content in groundwater is essentially related to gypsum dissolution and cation exchange processes and not to carbonate weathering.

The process of base exchange is confirmed by the diagram (Na–Cl) versus $[(Ca + Mg) - (HCO_3 + SO_4)]$ (McLean et al., 2000; Garcia et al., 2001; Dassi, 2004; Carol et al., 2009) (Fig. 6). In this diagram the water samples are aligned along a line of slope −1, show an inversely proportional change between Na^+, on the one hand, and Ca^{2+} and/or Mg^{2+} on the other hand. In the absence of these reactions, all samples should be placed near the point of origin (McLean et al., 2000).

The process of cation exchange between groundwater and its host environment is highlighted, by the calculated Base Exchange Indices, in particular the Chloro Alkaline Indices (CAI 1,2) (Garcia et al., 2001). These above indices are calculated using the following equations:

$$CAI1 = Cl - (Na + K)/Cl$$

$$CAI2 = Cl - (Na + K)/SO_4 + HCO_3 + CO_3 + NO_3$$

If there is exchange of K and Na from water with Ca and Mg of the rock, the exchange is direct, and both the indices are positive. If the latter values are negative, and then the exchange is indirect and therefore, there is an exchange of Mg and Ca of the waters with Na and K of the rocks. The groundwater samples showed positive indices, illustrating that they had direct base exchange reaction (Fig. 7).

The nitrate contents in the Grombalia groundwater fluctuate between 0.8 and 590 mg/l. Thirty-four samples show high nitrate contents exceeding 50 mg/l, the World Health Organization's (WHO's) recommended maximum for drinking-water (WHO, 2006). These high concentrations of nitrate are most likely related to the fertilizer application and long-term flood irrigation practices, highlighting the significant contribution of the return flow of irrigation waters to the degradation of groundwater quality (Singh et al., 1995; Oenema et al., 1998; Hadas et al., 1999).

Spatially, three groups of samples have been identified (Fig. 8):

- The first group is placed on the positive side of axis F2 and groups the most mineralized samples. This indicates that the

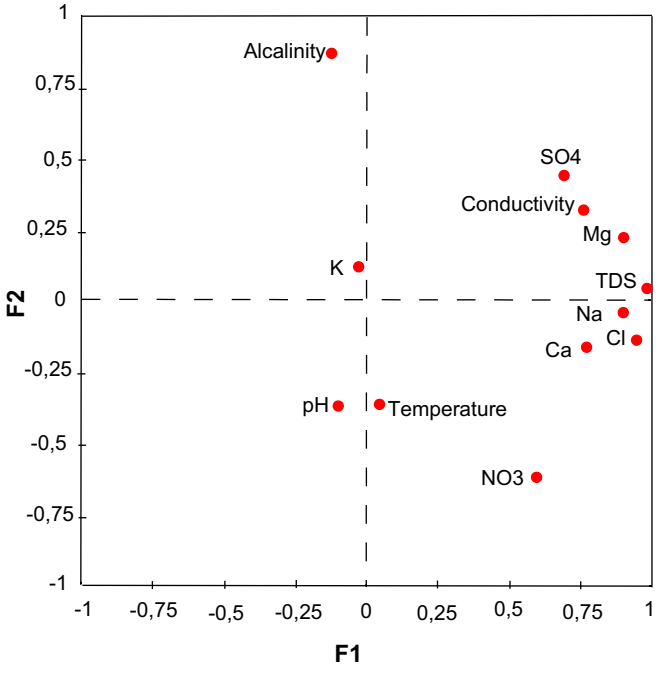

Fig. 5. Variable space deduced from the geochemical PCA.

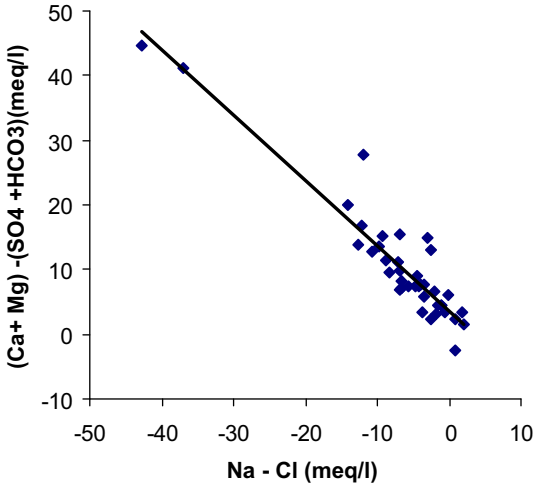

Fig. 6. Plot of (Na–Cl) versus $[(Ca + Mg) - (SO_4 + HCO_3)]$.

interaction of water with the host rock has played an important role in the acquisition of water salinity.

- The second group, which lies on the positive side of axis F1, is strongly associated with nitrate showing pollution related to agricultural practices. Indeed, the application of flood irrigation in parallel with the over-fertilization of cultivated perimeters led to increased nitrate leaching through the phenomenon of return of irrigation water.
- The third group is placed on the negative side of F1 and F2. It is strongly associated with pH and negatively correlated with nitrate reflecting the importance of the phenomenon of denitrification. This phenomenon contributes to transformation by bacterial NO_3 to N_2.

This dissolution is highlighted, through both the undersaturation state with respect to the halite, and the proportional parabolic evolution of the saturation indexes versus the sum of ions deriving from NaCl dissolution (Fig. 9).

The majority of groundwater samples indicating saturation state of calcite and dolomite (Table 4). Therefore, the mentioned minerals are not susceptible to dissolution. However, all groundwater samples show negative saturation indices, which indicate undersaturation with respect to gypsum and anhydrite, indicating the eventual dissolution of these sulphate minerals:

$$CaSO_4 \cdot 2H_2O \rightarrow Ca^{2+} + SO_4^{2-} + 2H_2O$$

Table 4
Saturation Index (SI) and isotopic data for the studied aquifers.

Well N°	$\delta^{18}O$	$\delta^{2}H$	^{3}H	SI					
	(‰ VSMOW)			Anhydrite	Aragonite	Calcite	Dolomite	Gypsum	Halite
1	−5.11	−28.9	4.6	−1.02	0.39	0.54	0.82	−0.8	−5.62
2	−4.84	−27.5	–	−1.04	0.12	0.26	0.56	−0.82	−5.66
3	−3.1	−28.2	4.1	−1.49	0.34	0.48	0.83	−1.27	−5.84
4	−5.33	−35.6	–	−1.37	0.33	0.47	0.83	−1.15	−5.61
5	−5.35	−29	–	−0.8	0.55	0.69	1.23	−0.59	−5.03
6	−5.19	−30.2	1.3	−1.42	0.45	0.59	1.17	−1.2	−5.44
7	−5.31	−31	–	−1.6	0.23	0.37	0.76	−1.38	−5.99
8	−3.75	−22.7	–	−0.84	0.81	0.95	2.05	−0.62	−4.7
9	−4.65	−28.4	–	−1.06	0.52	0.66	1.66	−0.84	−4.71
10	−5.01	−29.3	–	−0.83	0.5	0.64	1.67	−0.61	−4.94
11	−5.03	−30.1	–	−1.04	0.25	0.4	1.02	−0.82	−4.62
12	−4.73	−26.7	–	−0.63	0.45	0.6	1.45	−0.41	−4.79
13	−4.87	−29.8	–	−0.92	0.52	0.67	0.89	−0.7	−5.69
14	−4.29	−25.8	–	−0.69	0.68	0.82	1.46	−0.47	−5.44
15	−4.7	−27.8	–	−1.93	0.5	0.64	1.07	−1.71	−6.4
16	−4.42	−27	–	−0.79	0.49	0.64	1.09	−0.57	−5.25
17	−4.6	−35.4	2.2	−1.36	0.47	0.61	1	−1.14	−5.99
18	−4.1	−32.6	3.8	−1.12	0.42	0.57	0.83	−0.9	−5.26
19	−5.32	−29.8	–	−1.66	0.73	0.88	1.94	−1.44	−5.94
20	−3.8	−27.1	4	−1.17	0.28	0.43	0.79	−0.95	−5.21
21	−4.56	−28.3	–	−0.91	0.26	0.4	1.09	−0.69	−4.47
22	−4.51	−26	–	−0.95	0.75	0.89	2.15	−0.73	−4.68
23	−2.8	−24.2	3.5	−0.86	0.42	0.56	1.49	−0.64	−4.86
24	−4.18	−24.7	–	−0.84	0.35	0.49	1.07	−0.62	−5.27
25	−5.33	−31.7	–	−0.97	0.43	0.57	1.08	−0.75	−5.52
26	−3.9	−31.3	2.9	−1.02	0.34	0.48	0.85	−0.8	−5.27
27	−5.1	−29	–	−0.87	0.31	0.45	0.71	−0.65	−4.63
28	−4.43	−27.3	–	−0.78	0.63	0.77	1.49	−0.57	−4.64
29	−4.95	−30.8	3.7	−1.04	0.52	0.66	0.84	−0.82	−5.83
30	−4.9	−35	1.6	−1.26	0.39	0.54	1.07	−1.04	−5.47
31	−3.9	−29	3.5	−0.94	0.38	0.52	1.26	−0.72	−5.1
32	−4.84	−27.5	–	−0.94	0.55	0.7	1.48	−0.72	−5.23
33	−4.74	−27.9	–	−0.89	0.48	0.62	1.34	−0.67	−5.29
34	−4.93	−27.5	–	−0.98	0.22	0.37	0.63	−0.76	−5.22
35	−5.1	−29.1	–	−1.75	0.29	0.44	1	−1.53	−5.38
36	−5.55	−31.9	–	−1.12	0.82	0.96	1.7	−0.91	−5.66
37	−5.5	−30.4	2.6	−1.05	0.1	0.25	0.6	−0.83	−5.47
38	−5.16	−28.1	–	−1.57	0.14	0.28	0.5	−1.35	−5.48
39	−4.5	−28.1	–	−1.76	0.44	0.58	0.68	−1.54	−6.5

5.4. Correlations of major ions

Several bivariate diagrams were performed to determine the origins of the mentioned ions and the processes that control their concentrations in Grombalia groundwaters. In the Na versus Cl diagram (Fig. 9), the majority of samples show high correlation, suggesting that the same origin of sodium and chloride is likely related to the halite dissolution as shown in the following equation:

$$NaCl \cdot 2H_2O \rightarrow Na^{+} + Cl^{-} + 2H_2O$$

This dissolution is highlighted through the positive correlation of most samples in the plot of Ca versus SO_4 and the proportional parabolic trend observed in the correlation of the saturation indexes, with respect to the referred minerals, versus the sum of ions resulting from eventual dissolution (Kamel et al., 2005) (Fig. 10).

6. Isotopic composition of groundwater

6.1. Stable isotopes of water ($\delta^{18}O$ and $\delta^{2}H$)

Stable isotopes ($\delta^{18}O$, $\delta^{2}H$) have conservative properties and provide information on the groundwater recharge processes (Gat,

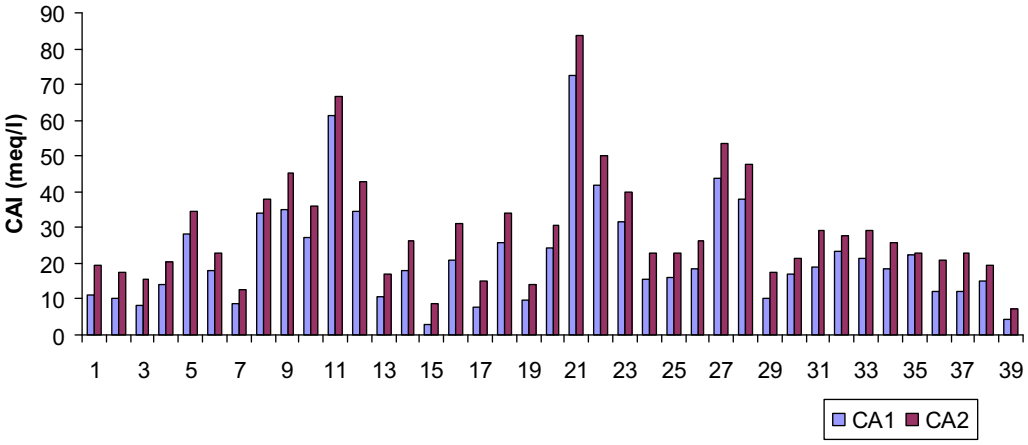

Fig. 7. CAI 1 and CAI 2 of groundwater samples.

1971). They can offer an evaluation of physical processes that affect water masses, such as evaporation and mixing (Geyh, 2000). The isotopic compositions of the groundwater samples from the Grombalia shallow aquifer range from −5.5‰ to −2.8‰ for $\delta^{18}O$ and from −35.6‰ to −22.7‰ for $\delta^{2}H$ (Table 4). The correlation diagram of $\delta^{18}O/\delta^{2}H$ (Fig. 11) shows the position of all samples relative to the Global Meteoric Water Line (GMWL: $\delta^{2}H = 8\ \delta^{18}O + 10$) (Craig, 1961) and the Local Meteoric Water Line of the Tunis-Carthage (LMWL: $\delta^{2}H = 8\ \delta^{18}O + 12.4$) (Zouari et al., 1985). Nevertheless, these groundwater samples can be further divided into three groups:

- The first group, characterized by the more enriched $\delta^{18}O$ and $\delta^{2}H$ contents. This indicates that they are not significantly affected by evaporation, which implies rapid infiltration of rainfall waters.
- The second group, which is placed below (or to the right of) the GMWL, comprises waters relatively enriched in ^{18}O and relatively depleted in deuterium with respect to the GMWL. This is probably the consequence of the infiltration of an evaporated component likely deriving from the return flow of irrigation water.
- The third group, placed between the GMWL and the LMWL, shows that the precipitation ensuring the recharge of the Grombalia aquifer originates from a mixture of oceanic and Mediterranean vapour masses (Maliki, 2000).

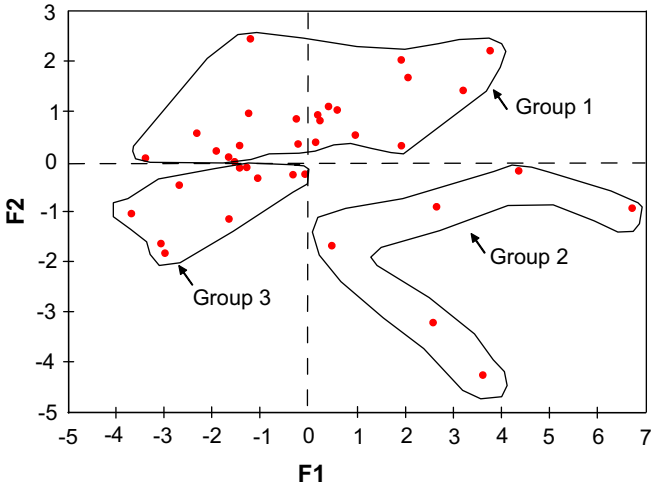

Fig. 8. Cluster analysis main sample groups according to their scores for F1 and F2.

In the diagram $NO_3/^{18}O$ (Fig. 12), the majority of samples show a positive correlation between these two elements. Thus, the return flow process in relation with the long-term flood irrigation practice contributes to mineralization by producing high amounts of nitrate. Some samples show an inverse proportional evolution. If denitrification is the main process for NO_3 removal, ^{18}O should become progressively more enriched as NO_3 is depleted (Boettcher et al., 1990; Aravena and Robertson, 1998; Mengis et al., 1999; Yuan et al., 2012). Thus, this may reflect the significance of denitrification.

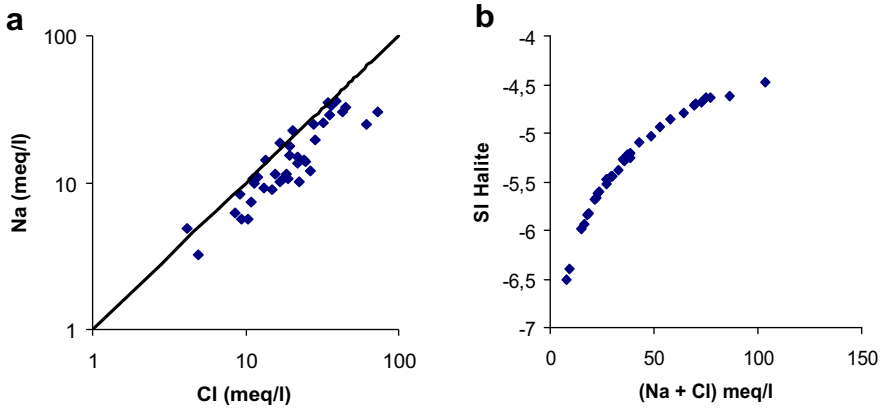

Fig. 9. Plot of Na versus Cl and (Na + Cl) versus SI of halite.

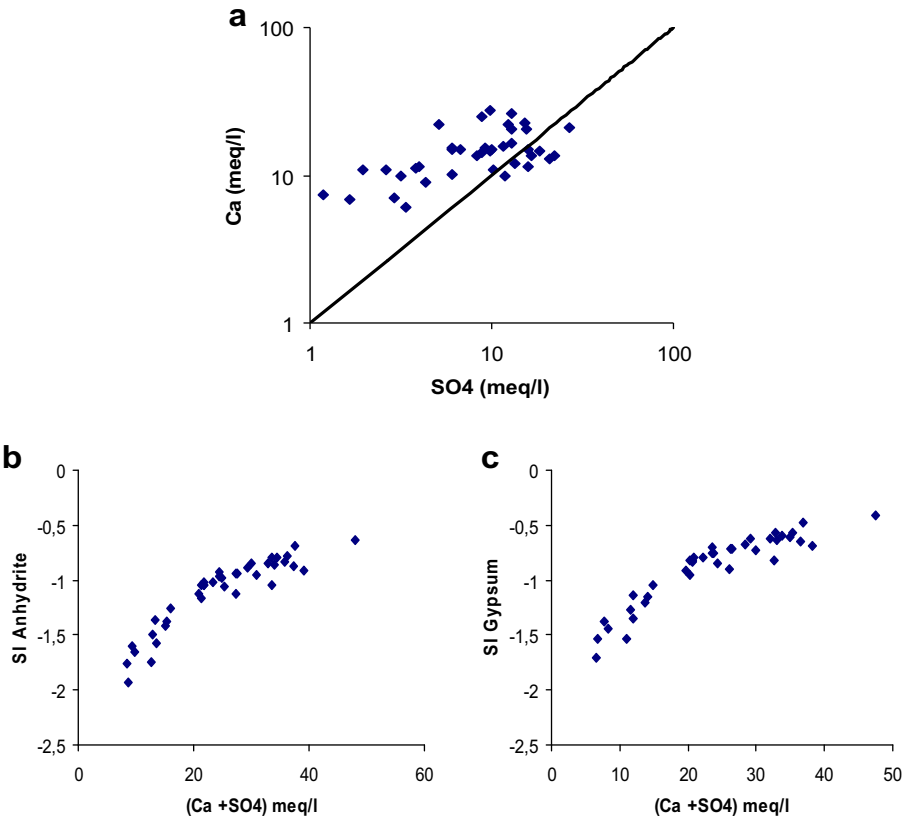

Fig. 10. Plot of Na versus Cl (a) and (Na + Cl) versus SI of halite.

The plot of chloride versus ^{18}O (Fig. 13) indicates the different processes responsible for the variation of groundwater salinity. Some water samples show a correlation between $\delta^{18}O$ and chloride, which confirms the contribution of evaporation in the mineralization. However, the majority of the samples show a poor correlation between these two elements. It is probable that the dissolution mechanism takes precedence over evaporation in the acquisition of the mineralization.

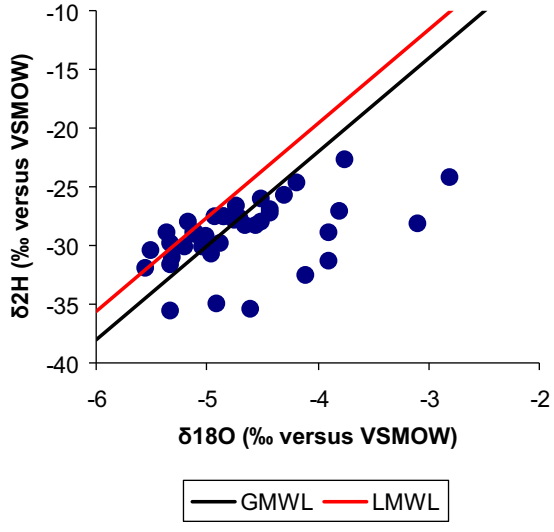

Fig. 11. $\delta^{18}O/\delta^{2}H$ diagram.

6.2. Radiogenic isotopes of water (^{3}H)

Tritium is a radioactive isotope of hydrogen that has a half life of 12.32 years (Lucas and Unterweger, 2000). In the 1950s and 1960s, the majority of tritium that was present in the atmosphere prior to thermonuclear testing was the result of natural production by the bombardment of nitrogen by neutrons in cosmic radiation in the upper atmosphere (Solomon, 2000). Between 1951 and 1980, tritium from anthropogenic atmospheric testing of nuclear weapons overwhelmed the natural cosmogenic origin (Plumner, 2005).

Considering the data of the tritium contents in precipitation collected in the Tunisian GNIP stations (Tunis-Carthage, no 6071500 and Sfax city, no 7622500) (Ben Moussa, 2011), the ^{3}H contents in groundwater from the study area, which vary from 1.3 to 4.6 TU

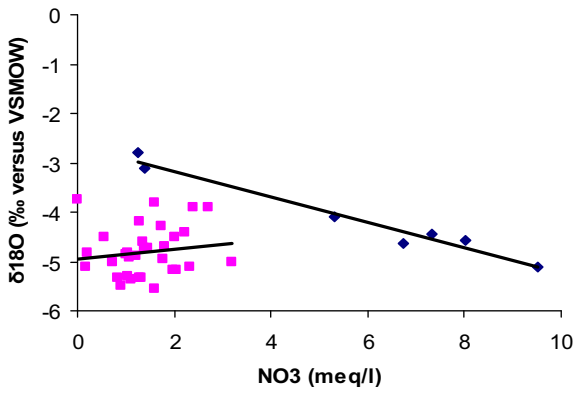

Fig. 12. Plot of NO_3 versus $\delta^{18}O$.

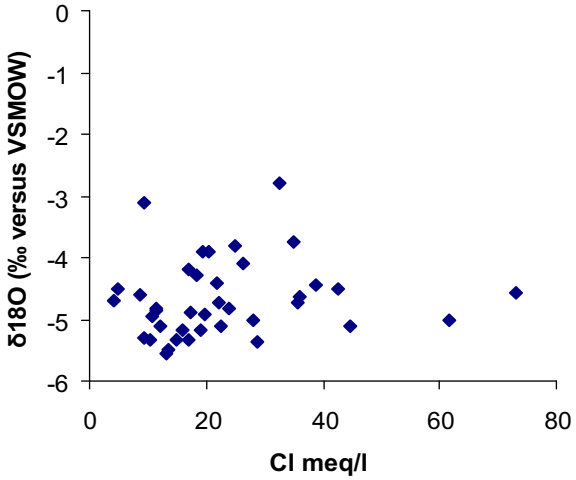

Fig. 13. Plot of Cl versus $\delta^{18}O$.

(Table 4), suggest two recharge periods. Waters with ^{3}H contents below 2 TU likely represent pre-nuclear recharge, i.e. recharge prior to thermonuclear testing in the 1950s and 1960s. However, waters with ^{3}H contents between 2 and 5 TU originate either from post-nuclear recharge, that infiltrated before nuclear weapon tests, or from recharge occurring during the last two decades.

7. Conclusion

This study reveals that coupling multivariate statistical techniques with hydrochemical analysis is an efficient way that allows discrimination between the different processes controlling the groundwater salinization in the Grombalia plain. The groundwater of Grombalia, divided into Na–Cl and Ca–SO_4–Cl water types, acquires its mineralization mainly through natural mineralization mechanisms such as the ion exchange and dissolution of evaporate minerals. Nevertheless, anthropogenic processes related to agricultural practices also play an important role in the salinization of groundwater.

The majority of samples of groundwater are characterized by high nitrate content, ranging from 0.8 to 590 mg/l. The combination of excess irrigation with over-fertilization has led to deleterious effects on the environment through water contamination and increased groundwater salinity. The TDS values of groundwater samples range from 0.75 to 5.6 g/l. Therefore, understanding the environmental consequences of agricultural practices is essential to minimize unexpected problems. The improvement of natural resources can be performed by evaluating the success of management practices in applying conservation policies needed to ensure long-term protection.

The stable isotope composition of water has permitted the identification of different types of waters in the aquifer of Grombalia. The tritium contents in groundwater from the study area confirm the recent infiltration and suggest two recharge periods of pre1950 and post1960.

Acknowledgments

The authors wish to thank the Laboratory of the International Agency of Atomic Energy (IAEA) for the financial support provided to the Technical Cooperation project (TUN 8/019) within which this work was carried out. Thanks are given to the staff members of Nabeul Water Resources Division/Agriculture Ministry.

References

Aravena, R., Robertson, W.D., 1998. Use of multiple isotope tracers to evaluate denitrification in ground water: study of nitrate from a large-flux septic system plume. Ground Water 36, 975–982.
Ben Ayed, N., 1993. Evolution tectonique de l'avant – pays de la chaîne alpine de la Tunisie du début du mésozoique à l'Actuel. Thèse d'Etat Université de Paris-11, Orsay.
Ben Moussa, A., Bel Hadj Salem, S., Zouari, K., Jlassi, F., 2010. Hydrochemical and isotopic investigation of the groundwater composition of an alluvial aquifer, Cap Bon Peninsula, Tunisia. Carbonates Evaporites 25, 161–176.
Ben Moussa, A., Zouari, K., Valles, V., Jlassi, F., 2012. Hydrogeochemical analysis of groundwater pollution in an irrigated land in Cap Bon Peninsula, North-Eastern Tunisia. Arid Land Research and Management 26, 1–14.
Ben Moussa, A., 2011. Etude hydrogéologique hydrochimique et isotopique du système aquifère de Hammamet Nabeul, Cap Bon, Tunisie Nord Orientale. Thèse de Doct., Univ. Sfax., 127 pp.
Ben Salem, H., 1995. Evolution de la péninsule du Cap Bon (Tunisie orientale) au cours du Néogène. Notes du Service Géologique de Tunisie 61, 73–84.
Boettcher, J., Strebel, O., Voerkelius, S., Schmidt, H.L., 1990. Using isotope fractionation of nitrate-nitrogen and nitrate-oxygen for evaluation of microbial denitrification in a sandy aquifer. Journal of Hydrology 114, 413–424.
Carol, E., Kruse, E., Mas-pla, J., 2009. Hydrochemical and isotopical evidence of 386 groundwater salinization processes on the coastal plain of Sambonombon Bay, 387 Argentina. J Hydrol 365, 335–345.
Castany, G., 1948. Les fossés d'effondrement de Tunisie, Géologie et hydrologie. Plaine de Grombalia et cuvettes de la Tunisie Orientale. 1er fasc. In: Ann. Mines. Géol. N°3, pp. 18–39.
Chen, K., Jiao, J.J., Huang, J., Huang, R., 2007. Multivariate statistical evaluation of trace elements in groundwater in a coastal area in Shenzhen. China. Environment Pollution 147, 771–780.
Chihi, L., 1995. Les fossés néogènes à quaternaires de la Tunisie et de la mer Pélagienne une étude structurale et une signification dans le cadre geodynamique de la méditerranée centrale. Thèse d'Etat, Université de Tunis II.
Coleman, M.L., Shepherd, T.J., Durham, J.J., Rouse, J.E., Moore, G.R., 1982. Reduction of water with zinc for hydrogen isotope analysis. Analytical Chemistry 54, 993–995.
Colleuil, B., 1976. Etude stratigraphique et néotectonique des formations néogènes et quaternaires de la région de Hammamet-Nabeul (Cap Bon) D.E.S. Université de Nice.
Craig, H., 1961. Standards for reporting concentrations of deuterium and oxygen-18 in natural waters. Science 133, 1833–1834.
Dassi, L., 2004. Etude hydrogéologique, géochimique et isotopique du système aquifère du bassin de Sbeitla (Tunisie Centrale). Thèse, University Sfax, Tunisie, 180 pp.
Davis, J.C., 1986. Statistics and Data Analysis in Geology. Wiley, New York.
DGRE Direction Générale des Ressources en eau, 1990. Annuaire piézométrique de la Tunisie DGRE. Tunis, Tunisie.
Epstein, S., Meyada, T.K., 1953. Variations of ^{18}O content of waters from natural sources. Geochimica et Cosmochimica Acta 4, 213–224.
Garcia, M.G., Del Hidalgo, M., Blesa, M.A., 2001. Geochemistry of groundwater in the alluvial plain of Tucuman province, Argentina. Hydrogeology Journal 9, 597–610.
Garcia, J.H., Arimoto, R., Okrasinski, R., Greenlee, J., Walton, J., 2004. Characterization and implication of potential fugitive dust sources in the Paso del Norte region. Science of the Total Environment 325, 95–112.
Gat, J.R., 1971. Comments on the stable isotope method in the regional groundwater investigation. Water Resources Research 7, 980–993.
Geyh, M.A., 2000. An overview of ^{14}C analysis in the study of groundwater. Radiocarbon 42 (1), 99–114.
Hadas, A., Sagiv, B., Haruvy, N., 1999. Agricultural practices, soil fertility management modes and resultant nitrogen leaching rates under semi-arid conditions. Agricultural Water Management 42, 81–95.
Hadj Sassi, M., Zouari, H., Jallouli, C., 2006. Contribution de la gravimétrie et de la sismique réfléxion pour une nouvelle interprétation géodynamique des fossés d'effondrement en Tunisie: exemple du fossé de Grombalia. Comptes Rendus Géoscience 338, 751–756.
Helena, B., Pardo, R., Vega, M., Barrado, E., M Fernandez, J., Fernandez, L., 2000. Temporal evolution of groundwater composition in an alluvial aquifer Pisuerga River, Spain by principal component analysis. Water Research 34 (3), 807–816.
Kaiser, H.F., 1960. The application of electronic computers to factor analysis. Educational Psychology Measurement 20, 141–151.
Kamel, S., Dassi, L., Zouari, K., Abidi, B., 2005. Geochimical and isotopic investigation of the aquifer system in the Djerid–Nefzaoua basin, southern Tunisia. Environmental Geology 49, 81–95.
Kumar, M., Ramanathan, A.L., Rao, M.S., Kumar, B., 2006. Identification and evaluation of hydrochemical processes in the groundwater environment of Delhi, India. Environmental Geology 50, 1025–1039.
Liu, C.W., Lin, K.H., Kuo, Y.M., 2003. Application of factor analysis in the assessment of groundwater quality in a blackfoot disease area in Taiwan. Science of the Total Environment 313, 77–89.
Lucas, L.L., Unterweger, M.P., 2000. Comprehensive review and critical evaluation of the half life of tritium. Journal of Research, National Institute of Standards and Technology 105 (4), 541–549.

Maliki, M.A., 2000. Etude hydrogéologique hydrochimique et isotopique de la nappe profonde de Sfax. Tunisie. Thèse de Doct., Univ. Tunis II, 254 pp.
McLean, W., Jankowski, J., Lavitt, N., 2000. Groundwater quality and sustainability in alluvial aquifer, Australia. In: Sililoo, O., et al. (Eds.), Groundwater, Past Achievement and Future Challenges. Balkema, Rotterdam, pp. 567–573.
Mengis, M., Schif, S.L., Harris, M., English, M.C., Aravena, R., Elgood, R.J., Maclean, A., 1999. Multiple geochemical and isotopic approaches for assessing ground water NO_3^- elimination in a riparian zone. Groundwater 37, 448–457.
Oenema, O., Boers, P.C.M., Van Erdt, M.M., Fraters, B., Van der Meer, H.G., Roest, C.W.J., Schroder, J.J., Willems, W.J., 1998. Leaching of nitrate from agriculture to groundwater: the effect of policies and measures in the Netherlands. Environmental Pollution 102, 471–478.
Piper, A.M., 1944. A graphic procedure in the geochemical interpretation of water-analyses. Transactions, American Geophysical Union 25, 914–923.
Plumner, L.N., 2005. Dating of young groundwater. In: Aggarwal, P.K., Gat, J.R., Froehlich, K.F.O. (Eds.), Isotopes in the Water Cycle: Past, Present and Future of a Developing Science. IAEA, Springer, Vienna, Netherlands, p. 381.
Pulido Leboeuf, P., 2004. Seawater intrusion and associated processes in a small coastal complex aquifer (Castell de Ferro, Spain). Applied Geochemistry 19, 1517–1527.
Schoeller, H., 1939. Le quaternaire du Golfe ancien de Grombalia. Tunisie. Actes Société Linnéenne de Bordeaux 91, 14–30.
Singh, B., Singh, Y., Sekhon, G.S., 1995. Fertilizer-N use efficiency and nitrate pollution of groundwater in developing countries. Journal of Contaminant Hydrology 20, 167–184.
Solomon, D.K., 2000. ^{3}H and ^{3}He. In: Cook, P.G., Herczeg, A.L. (Eds.), Environmental Tracers in Subsurface Hydrology. Kluwer, Boston, pp. 397–424.
Taylor, C.B., 1977. Tritium Enrichment of Environmental Waters by Electrolysis: Development of Cathodes Exhibiting High Isotopic Separation and Precise Measurements and Applications. High Tartras, Czechoslovakia, October 1975, Bratislava.
WHO (World Health Organization), 1993. Guidelines for Drinking Water Quality. In: Recommendations, second ed., vol. 1. WHO, Geneva, 130 pp.
World Health Organization (WHO), 2006. Guidelines for Drinking Water Quality. Incorporating First Addendum, third ed., http://www.who.int/water_sanitation_health/dwq/gdwq3rev/en/index.html (accessed 2009).
Yuan, L., Zonghe, P., Tianming, H., 2012. Integrated assessment on groundwater nitrate by unsaturated zone probing and aquifer sampling with environmental tracers. Environmental Pollution 171, 226–233.
Zouari, K., Aranyossy, J.F., Mamou, A., Fontes, J.Ch., 1985. Etude isotopique et géochimique des mouvements et de l'évolution dessolutions de la zone aérée des sols sous climat semi-aride (Sud tunisien). In: Stable and Radioactive Isotopes in the Study of the Unsaturated Soil Zone, IAEA-TECDOC-357, Vienna, pp. 121–144.